Spectroscopy and Potential Energy Surfaces

C. M. Western
School of Chemistry, University of Bristol, Cantock's Close, Bristol BS8 1TS, U.K.

1 Introduction

Potential energy surfaces are fundamental to chemistry; if you know the potential energy surface for a system many of its properties can be calculated from it. The forces acting within and between molecules are often discussed in a qualitative way when interpreting the behaviour of molecules, such as interpreting the behaviour of mixtures of liquids in terms of the interactions between like and unlike molecules. A quantitative understanding is also possible, given appropriate measurements or calculations, and this is the area I intend to discuss in this review. I am going to concentrate on simple systems, involving just a few atoms, as it is on these systems that very detailed measurements can be made and a complete map of the potential energy surface can be put together. It is also possible to calculate all the properties of such systems from first principles to compare with experiment. Such calculations are not routine, being very time consuming, and ones that can reproduce all the experimental data to the experimental accuracy are few and far between. The increase in complexity as we go to larger systems is such that we must limit ourselves to less detailed experiments and calculations, but work on smaller systems can give guidance as to what models will work and where approximations can be made.

It is not possible to measure potential energy surfaces directly; some property must be measured that depends on the potential energy surface and a model potential is adjusted to make the property agree with experiment when calculated from the model potential. The measurements that yield the most detailed information on a potential energy surface are almost invariably spectroscopic ones, and in this review I will be giving an overview of modern spectroscopic studies on isolated, small molecules which have yielded important information on potential energy surfaces. In a sense this review could also have been entitled 'Modern Applications of Laser Spectroscopy', because recent developments have typically involved the use of (one, or more often, several) lasers. The techniques used are usually not new (though there are some important new refinements), but over the past decade or so laser technology has become sufficiently mature and stable that difficult systems can be tackled, rather than those which are just operationally convenient. For this reason I will concentrate on the results, rather than the hardware, and below I hope to give the flavour of the important measurements that can be made today and the results that can be obtained from them. As the topic is so wide the selection I make must be arbitrary; areas I have completely ignored include dynamical studies and investigations of larger molecules, as reviews of these areas have appeared recently in this journal.[1,2]

Dr. Western studied for his first degree at St. John's College, Oxford, going on to take his D.Phil. under Dr. B. J. Howard in the field of Van der Waals complexes. He then spent two years at the California Institute of Technology with Professor K. C. Janda. He returned to the U.K., to Bristol, initially as a postdoctoral fellow, then as a Royal Society 1983 University Research Fellow, and finally as a Lecturer. During this time he has been working on electronic spectroscopy of many molecules using a wide variety of laser based techniques.

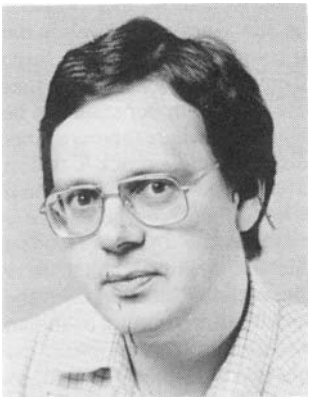

2 Determining the Potential Energy Surface

As the link between spectra and the potential energy surface is not trivial I will start by going through the process for a diatomic molecule. This serves to illustrate the principles involved, though a lot of extra complexity is introduced on going to a triatomic or larger molecule. It also indicates what experiments are required to determine the potential energy surface completely.

First, suppose we have a well-resolved spectrum; Figure 1a shows a simulation of part of the visible electronic spectrum of I_2, the $B^3\Pi_{0+u} - X^1\Sigma_g^+$ transition, with both rotational and vibrational structure visible. A complete picture of this spectrum can be found in the Iodine Atlas[3] as this spectrum is often used for calibration purposes. The spectroscopist can assign each transition in terms of the vibrational and rotational quantum numbers involved and then produce spectroscopic constants that reproduce the observed transitions for each vibrational band. In this case the procedure is straightforward, though time-

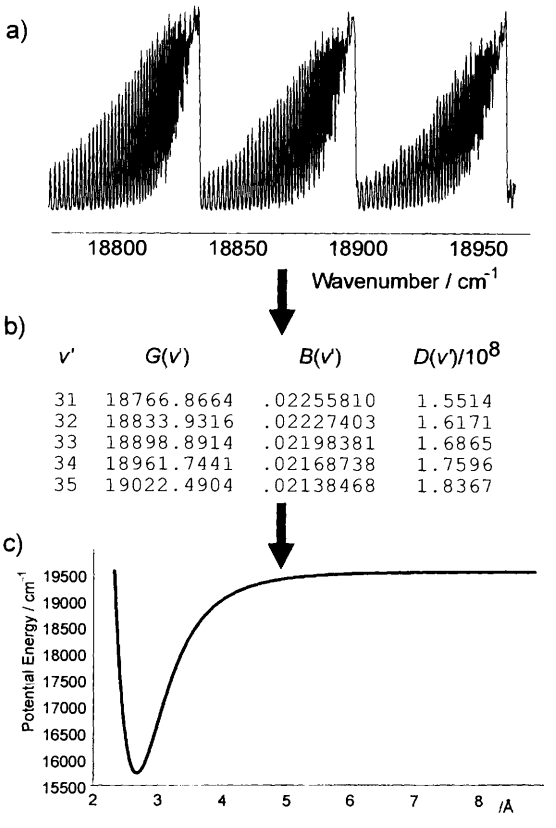

Figure 1 Determination of the potential energy curve for I_2. (a) Simulation of a fragment of the visible spectrum; the temperature was set at 100 K so that the structure of the spectrum in clear. (b) Spectroscopic constants derived from (a). (c) Potential energy curve for the *B* state of I_2.

consuming, as the rotational energy levels for each vibrational level (with quantum number v) follow the simple formula in terms of the rotational quantum number J

$$E(v,J) = T_v + B_vJ(J+1) - D_vJ^2(J+1)^2 + \quad (1)$$

The resulting table of rotational constants (B_v, D_v) and band origins T_v (Figure 1b) can be further reduced by expressing the constants as power series in $v+\frac{1}{2}$ such as

$$G(v) = \nu(v+\tfrac{1}{2}) - x\nu(v+\tfrac{1}{2})^2 + \quad (2)$$

$$B(v) = B_e - \alpha(v+\tfrac{1}{2}) + \quad (3)$$

ν is the vibrational stretching frequency These formulae (or tables) can be extended to cover a wide range of levels in the excited state and provides the input to the final stage, the determination of the potential energy surface For diatomic molecules the RKR (Rydberg–Klein–Rees) method can be used[4] to give the classical turning points, r_+ and r_-, (the points on the curve where the potential energy equals the total energy) for each of the observed vibrational levels

$$r_+ - r = \sqrt{\frac{h}{32\pi^2 c\mu}} \int_{\frac{1}{2}}^{v} \frac{dv'}{\sqrt{G(v) - G(v')}} \quad (4)$$

$$\frac{1}{r} - \frac{1}{r_+} = \sqrt{\frac{2\pi^2 c\mu}{h}} \int_{\frac{1}{2}}^{v} \frac{B(v')dv'}{\sqrt{G(v) - G(v')}} \quad (5)$$

These two equations give the full potential energy curve for the excited state, as shown in Figure 1c The RKR method is in fact a semi-classical method but it is accurate and easy to apply, the computer program required to evaluate equations 4 and 5 is only 200 or so lines of FORTRAN[5] and is not beyond the capabilities of a large pocket calculator

For polyatomic molecules each step in the process

taking spectra → molecular constants → potential energy surface

becomes much more complicated because of the greater number of degrees of freedom For a triatomic molecule there are three modes of vibration and thus three vibrational coordinates (or four if the molecule is linear) and even plotting the potential energy surface becomes difficult as a 3D picture can only show two coordinates If the molecule is not linear the rotational picture will also be more complicated as the molecule becomes a symmetric or asymmetric top These effects make even the first step, taking spectra, more difficult as a polyatomic molecule will have many more states populated at any given temperature and thus more congested and overlapped spectra The spectra will also be weaker as the same intensity is shared over more transitions

The molecular beam techniques described below are invaluable in counteracting these problems by reducing the number of states populated The consequent reduction in the number of transitions also helps in the next stage, assigning the spectrum The extraction of spectroscopic constants from the spectrum is also more difficult as the model Hamiltonians are more complicated, but the use of computers means that this is not an overwhelming problem

The final stage, the reduction to the potential energy surface, is much more tricky for polyatomics as there is no equivalent to the RKR procedure to allow a direct inversion of the spectroscopic data to the potential energy surface Instead an alternative scheme must be used, outlined in Figure 2 This involves the expression of the potential energy surface in terms of various adjustable parameters, rather than a simple numerical tabulation as produced by the RKR process The experimental spectra (or the spectroscopic constants derived from them) are then calculated from this surface using estimated initial values for the parameters The results are compared with experiment and the parameters adjusted on the basis of this comparison This process is repeated until a reasonable match with experiment is

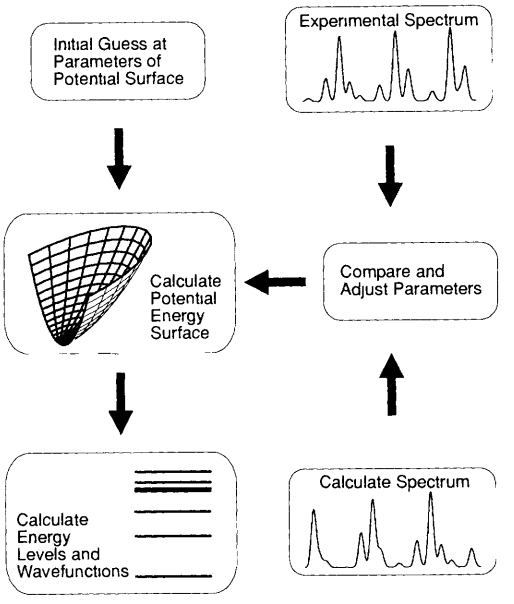

Figure 2 Flow diagram for determining polyatomic potential energy surfaces by adjusting the parameters defining the surface

achieved The programs involved are large, as calculations of energy levels on a general potential energy surface are complex and time-consuming This is particularly true as we are concerned with the complete potential energy surface and conventional methods relying on approximations such as the harmonic oscillator are only valid in the equilibrium region In fact, most of the molecules mentioned in this review have unusual features in their potential energy surface which give calculation problems even in the equilibrium region We will not discuss this computational problem further here, but refer the reader elsewhere [6,7] We merely note that, while significant computer resources are required, they are typically much less than those required for a complete *ab initio* calculation of the surface

Despite the extra complexities of polyatomic molecules the diatomic picture does indicate which energy levels must be measured and which experiments can probe those levels Equations 4 and 5 indicate that determination of the turning points for a particular vibrational wavefunction requires a knowledge of all the vibrational and rotational levels up to that level In practice much progress can be made with only limited rotational information when using a model potential function with adjustable parameters The equilibrium geometry is required but the use of physically reasonable potentials can constrain the possible form of the potential sufficiently that the rotational information is not absolutely essential Its omission can, however, lead to ambiguities in the resulting potential Either way, measurement of a wide range of vibrational levels is essential for determination of the potential energy surface over a wide range of geometries so we must consider the levels accessible to spectroscopy For the I_2 example described above there were no restrictions, starting from the lowest few vibrational levels in the ground state that are populated at room temperature, the large change in geometry upon electronic excitation means that essentially all of the vibrational levels of the upper state can be seen The situation is as shown in Figure 3a, where there is a large change in geometry on excitation so that the Franck–Condon factors are favourable for large changes in the vibrational quantum number, v On the other hand, in cases where there is no change in geometry on excitation the Franck–Condon factors will be very unfavourable for a large change in v rendering most upper state levels inaccessible starting from the room temperature distribution over vibrational states, as shown in Figure 3b There are various ways round this problem, the obvious one of heating the sample is a possibility though, as indicated by our advocating the use of low temperatures to avoid

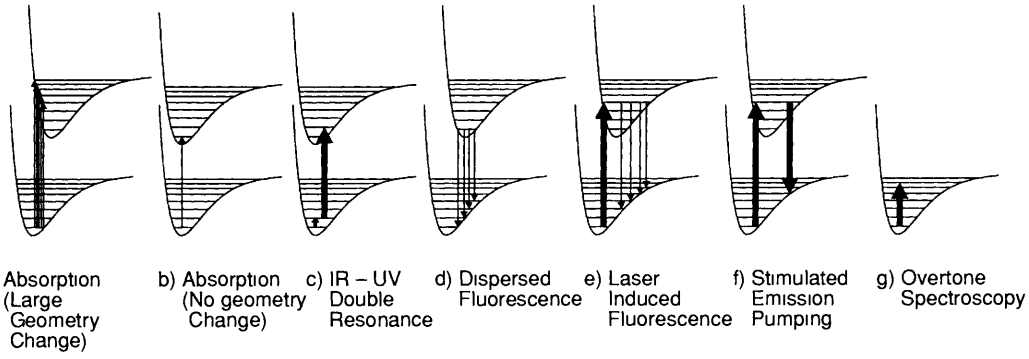

Figure 3 Spectroscopic schemes used for the determination of potential energy surfaces Laser-driven transitions are indicated with a thick arrow

congestion, this also introduces problems An alternative method is the use of a laser to excite a vibrational transition in the ground state prior to the electronic excitation, as shown in Figure 3c This is an example of *double resonance*, specifically infrared–ultraviolet double resonance (IR-UV DR) and we illustrate its application below to NH_3 The possible transitions within the ground state are, however, limited and another possible double resonance technique is to go *via* a different electronic state with a different geometry so the Franck–Condon factors again become favourable for large changes in v This is in fact how the ground state levels for I_2 can be mapped out as shown in Figure 3d Starting from a single level of the upper electronic state a wide range of lower state levels can be measured by analysing the fluorescence emitted from this state Such excited states can be prepared by various means, including chemical reactions and electric discharges, but in view of the requirement for simple spectra the use of a laser in the first step, Figure 3e, will give the best results The technique of *Stimulated Emission Pumping* (SEP), Figure 3f uses the same basic energy level scheme but stimulates the final downward transition rather than relying on spontaneous fluorescence This gives some important advantages, as described below Finally, it is worth noting that, while vibrational transitions involving large changes in v (Figure 3g) are in general very weak, such transitions can be seen for very anharmonic vibrations of which hydrogen stretching vibrations (C–H, O–H) are the best example An example of work on these *overtone* transitions is described below for HCN

3 Molecular Beams

No review of modern high resolution spectroscopy would be complete without mention of molecular beams [8] These provide gas samples at a temperature of a few K with reasonable number density (equivalent to 1 Torr at room temperature) Such low temperatures make them invaluable for simplifying complex spectra and the combination of low temperature and high pressure make them ideal for studying Van der Waals complexes, which we discuss in detail at the end of the review This seemingly impossible combination is actually quite easy to produce in practice, the basic apparatus (Figure 4) consists of a vacuum chamber with a small hole to allow the sample gas (at atmospheric pressure or above) to enter Providing the hole is larger than the mean free path of the gas molecules the resulting jet of gas has some unusual properties All the molecules within the jet are moving with similar velocity, giving little relative motion of the molecules To a molecule within the jet this is equivalent to a low temperature, though in fact no energy has been removed from the gas, all the random thermal motion of the molecules has been converted into kinetic energy in one direction This state of affairs comes about by a 'natural selection' type of process – molecules that are not travelling in the right direction, or with a different speed to the average, are more likely to experience a collision that will change their velocity This collisional mechanism also gives efficient rotational cooling though the process is too fast to provide good relaxation of the more widely separated vibrational and electronic energy levels These molecular beams are often referred to as supersonic jets, as the speed of the molecules in the jet is much faster than the local speed of sound in the jet (which is low because there are so few collisions) Figure 5 shows an example of the great simplification made possible with these supersonic jets, showing the vast difference between a room temperature spectrum and a 10 K spectrum It also shows another important advantage – not only is the spectrum simpler, but weak features, such as the $\tilde{B}2^2 4^2$ band, that are obscured at room temperature become clearly visible at low temperatures The importance of the advantages of supersonic jet spectroscopy is shown by the fact that most of the work described in this review was carried out in a molecular beam

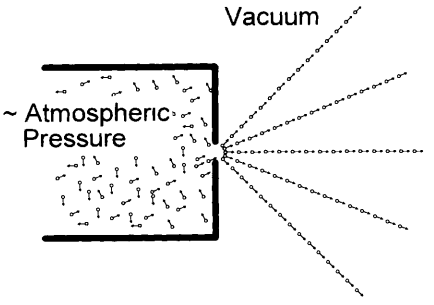

Figure 4 Schematic of a molecular beam

4 Excited Electronic States

The sample spectrum from the last section is from our first case study, on the $\tilde{B}^1E''$ state of NH_3 [9] It is actually a multiphoton[10] spectrum, arising from the simultaneous absorption of two photons, but for the purposes of this review this can simply be looked on as an alternative way of taking electronic spectra, as it does not affect the Franck–Condon factors The excited state arises from the promotion of one of the lone pair electrons on N to a degenerate $3p_{x,y}$ Rydberg orbital In common with other excited states of NH_3, removal of one of the lone-pair electrons removes the factor bending the molecule and the molecule becomes planar The interesting feature of this state is that it is degenerate, and may thus be subject to a Jahn–Teller distortion lowering the symmetry This distortion is indeed present, though small, and to investigate this in detail requires a knowledge of the vibrational modes inducing the distortion, the degenerate asymmetric modes ν_3 (N–H stretch) and ν_4 (in-plane bend) However, as there is effectively no change in these modes on excitation they are difficult to see in a conventional electronic spectrum, *i e* for these modes the picture is as in Figure 3b Figure 5 shows how a low temperature spectrum can render visible the weak transitions involving these modes, in this case a change of 2 quanta in ν_4 Note how weak this transition is in contrast to the neighbour-

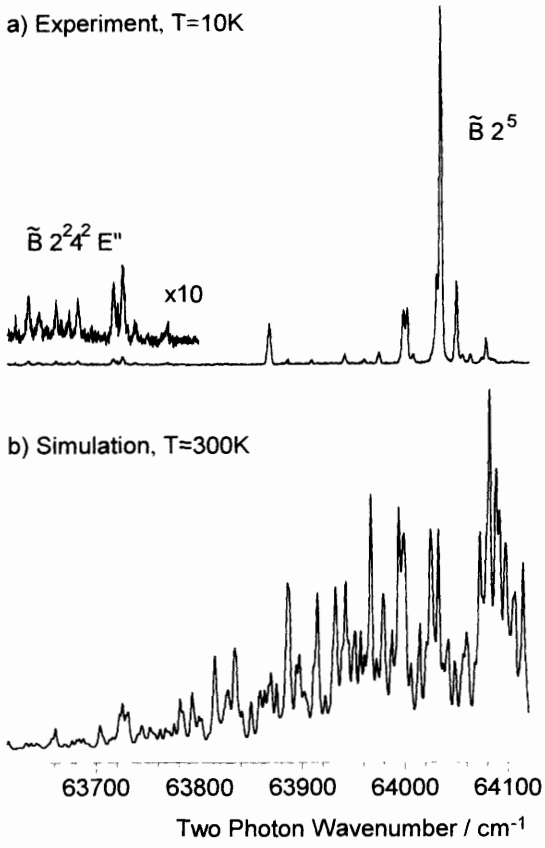

Figure 5 Electronic spectrum of NH_3: (a) as seen in a molecular beam at 10 K, (b) simulation of equivalent room temperature spectrum.

ing 2^5 transition (the notation implies ν_2 changes to $v_2 = 5$ from $v_2 = 0$, with the other modes unchanged). For ν_2, the umbrella motion, the picture is as in Figure 3a because of the change in geometry to planar from pyramidal.

These weak transitions provide some information on the modes of interest, but not enough, partly because of symmetry restrictions. The infra-red ultraviolet double resonance scheme shown in Figure 3c can get round this restriction by exciting the degenerate modes of interest in the ground state. The Franck–Condon factors then act to preserve the vibrational motion on excitation to the excited electronic state.

Figure 6 shows a typical double resonance spectrum; here an infra-red laser (the *pump* laser) excites a single rotational transition within the $\nu_2 + \nu_3$ band in the ground state and a second (ultraviolet) laser (the *probe* laser) takes an electronic spectrum of this vibrationally excited state. The figure illustrates two features of double resonance spectroscopy. The first feature, a great advantage, is that the double resonance spectra are very simple. This is because a single rotational level is prepared in the intermediate state from which only a few transitions are possible. In the simplest cases a single rotational level will yield just two transitions in double resonance, corresponding to the two possible changes in J (+1 and −1). If the assignment of the first transition is known, assignment of the final state quantum numbers is trivial. The second feature of double resonance spectroscopy is obvious from Figure 6 – ordinary (single resonance) transitions induced by one of the lasers (in this case the probe laser) provide an awkward background. Figure 6a shows such a spectrum, produced by the probe laser only. This is a common problem in double resonance and some ingenuity can be required to remove these unwanted single resonances. In this case two spectra are recorded simultaneously, using two identical sample cells with only one (shown in Figure 6b) exposed to the first (infrared) laser beam and the difference, as shown in Figure 6c, reveals the double resonant transitions.

The results for this study give a reasonable selection of the

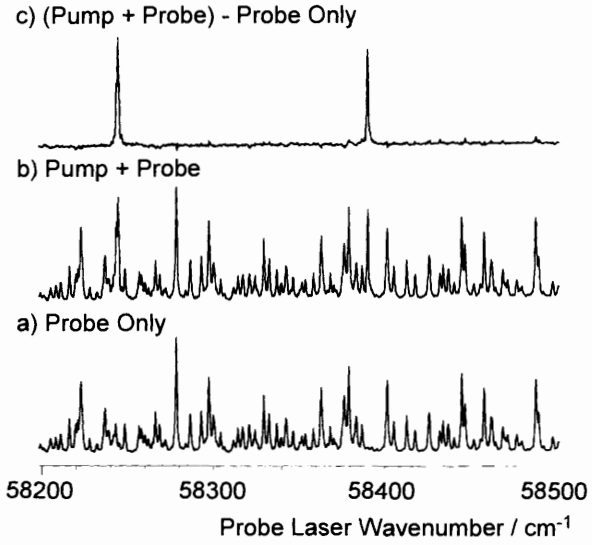

Figure 6 Infrared ultraviolet double resonance spectrum of NH_3. The three spectra are: (a) from the probe laser only, (b) from both the pump and probe lasers, and (c) the difference between (a) and (b) showing the double resonance transitions only.

lower vibrational levels involving ν_3 and ν_4. The potential energy surface for NH_3 is actually quite complicated, involving 6 vibrational coordinates, and we cannot claim that the surface is known in its entirety. We will look at just the two coordinates involved in ν_3, the doubly degenerate asymmetric stretch. These arise from the two coordinates required to describe the three N–H bond lengths after removing the symmetric stretch (ν_1) corresponding to changing all bonds equally. In the absence of the Jahn–Teller distortion the potential energy as a function of these two coordinates will look something like Figure 7a, a simple circular bowl corresponding to an identical simple harmonic well along each coordinate. As the electronic state is degenerate there will be two identical such bowls, one for each component. The presence of the Jahn–Teller effect mixes the two surfaces, with the mixing increasing linearly with the displacement from the centre. This lifts the degeneracy between the two electronic states and the lower of the pair now has a minimum away from the centre, Figure 7b, though the potential still has circular symmetry. An important conclusion from this work was that mixing with other electronic states is as important as the Jahn–Teller effect in determining the vibrational energy levels; this mixing is with non-degenerate electronic states and has the effect of destroying the circular symmetry, Figure 7c. Both these effects are quite small in this case as the depth of the Jahn–Teller induced well is less than the zero-point energy in this mode so the average structure is still symmetrical.

For another example of double resonance see the work of Crim *et al.* on the $\tilde{A}$ state of acetylene.[11] Here double resonance allowed *u* (asymmetric) vibrations to be seen for the first time in the excited state, prompting a significant reanalysis of the vibrational structure.

5 Ground Electronic States

We now turn to methods of looking at ground state potential energy surfaces. We illustrate this with work on HCN as this provides an excellent example of work with two important techniques. The end result[7] is one of the most complete determinations of the potential energy surface for a triatomic molecule available to date, covering vibrational energies up to 25000 cm^{-1} though, unfortunately, the highly excited bending states at 17000 cm^{-1} and above (which are expected to isomerize to HNC) have not yet been observed. As implied by the introduction, this has required the measurement of highly excited vibrational states over a wide range of energies.

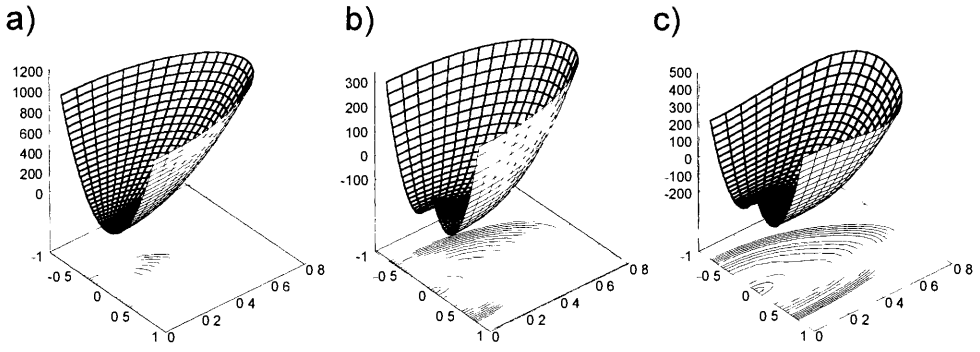

Figure 7 Model potential energy surfaces for the $\tilde{B}$ state of NH_3: (a) with no Jahn–Teller distortion, (b) with a Jahn–Teller distortion, (c) including mixing with other electronic states.

5.1 Overtone Spectroscopy

HCN is one of the cases where vibrational spectroscopy can give some high vibrational levels directly, as high overtones of the C–H stretching vibrations have been observed. These overtones extend into the visible and almost into the ultraviolet in marked contrast to normal vibrational transitions which are restricted to the infrared; for HCN, levels with up to 8 quanta of stretching vibration at 23 000 cm^{-1} have been observed.[12] These overtones are very weak; the absorptions in the visible are not enough to make the HCN gas coloured, but they can be seen if sensitive multi-pass methods are used. The work mentioned[12] involves a new development in long path methods, cavity ring down absorption. This technique involves a pair of highly reflective, parallel mirrors forming an optical cavity. A laser beam passing through this cavity will be reflected back and forwards many times before exiting, giving effective path lengths up to 70 km with a one metre cell. The novel twist in this method is the measurement of the decay time of the light exiting from the cell rather than its intensity. Even for a short laser pulse (typically 10 ns for the lasers used here) the output from the cell persists for several tens of microseconds as the light pulse is reflected back and forth within the cell. Absorption in the cell will make the light output decay faster as more light will be removed in each pass. Measuring this decay time is preferable to simply measuring the intensity loss in the cell as lasers, particularly pulsed lasers, have poor intensity stability making small changes hard to see. Measuring the rate of decay for each laser shot is not affected by any variation in intensity, so much smaller absorptions can be seen. Figure 8 shows a spectrum of the $\nu_1 + 6\nu_3$ overtone of HCN taken in this way.

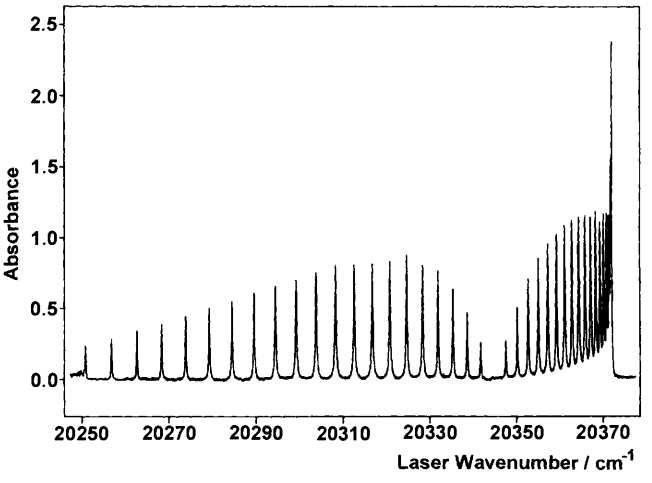

Figure 8 Cavity absorption overtone spectrum of HCN.
(Reproduced by permission from *J. Chem. Phys.*, 1993, **99**, 6287.)

5.2 Stimulated Emission Pumping (SEP)

These overtone transitions are, however, almost entirely restricted to stretching transitions and give no information as to the bending potential. This restriction can be removed by going through a different electronic state using the schemes in Figure 3e and 3f. For HCN the $\tilde{A}$ state is ideal for this purpose as not only is the CN bond longer than in the ground state (1.3 Å as compared to 1.15 Å) but also the equilibrium geometry is bent, with an equilibrium bond angle of 125°. The two-step process involved in stimulated emission pumping[13,14] has allowed levels with up to 14 quanta of bending vibration[15] to be observed in HCN. The principle of this technique (Figure 3f) is as follows: one laser (the PUMP laser) is used to prepare a single rovibrational level in the excited electronic state. The spontaneous fluorescence from this level is monitored while a second laser (the DUMP laser) is scanned over the region of interest. On resonance the DUMP laser stimulates emission down to ground state levels and causes a drop in the monitored spontaneous emission (as the stimulated emission comes out parallel to the DUMP laser and will not reach the fluorescence monitor mounted perpendicular to the laser beams). The spectra obtained for HCN are similar to the simpler of the spectra illustrated below for CH_3O (Figure 9) showing the very simple

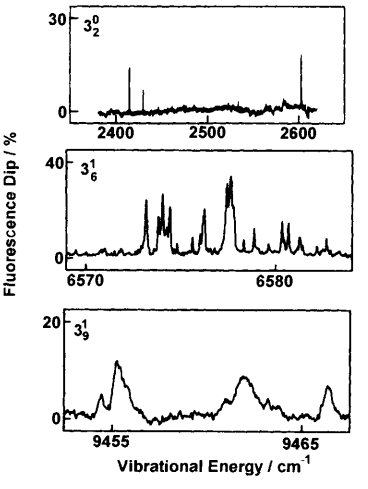

Figure 9 Stimulated emission pumping spectra of CH_3O at various levels of vibrational excitation in the ground state.
(Reproduced by permission from *J. Chem. Phys.*, 1994, **101**, 3618.)

form we saw above for double resonance spectra. There are two important points to be made about this technique. First, this technique is limited by fluctuations in the pump laser intensity as these limit the reduction in fluorescence that can be seen. Even with the difference techniques commonly used the minimum measurable depletion is normally no less than 1%. On the other hand, the resolution of this technique is very good, being limited only by the resolution of the lasers used. This is in marked contrast to the older method of wavelength analysing the

spontaneous fluorescence with a monochromator (Figure 3e) as here high resolution requires the monochromator slits to be set very narrow, giving very low signals Furthermore the laser intensity can normally be greatly increased to stimulate very weak transitions without problems, the modern pulsed dye lasers used for SEP can typically offer 100–1000 times the power required to saturate strong transitions The net result of this is the measurement of a very wide range of vibrational levels of HCN leading to the potential energy surface determination mentioned above [7]

As a further example of what is possible consider the work by Geers *et al* [16] on the ground ($\tilde{X}^2E$) state of CH_3O Like the $\tilde{B}$ state of NH_3 discussed above it is subject to a small Jahn–Teller distortion, though this is not yet fully analysed Instead we will discuss some other aspects of the potential energy surface that are likely to be important for any molecule SEP has been performed *via* the $\tilde{A}^2A_1$ state, this arises from the promotion of a C–O σ bonding electron to a lone pair on O, giving an increase in the C–O length of 0 2 Å This gives a long progression in ν_3'', the ground state C–O stretching mode, in the SEP spectrum The spectrum shows some interesting features when the individual peaks in the progression are examined at high resolution, Figure 9 (The energy scale in these figures is the energy of the final ground state level reached, being the difference between the PUMP and DUMP lasers) At low levels of vibrational excitation a very simple spectrum is seen with just a few rotational lines as we expect for a double resonance technique Above 5000 cm^{-1} there is a sudden increase in the number of lines seen but the observed linewidth does not start increasing until ~9000 cm^{-1} The extra lines are due to additional rovibrational transitions indicating that the selection rules on K and v have broken down (The selection rule on J remains rigorous) Estimates of the density of states (around 5–10 per cm $^{-1}$ at 6500 cm^{-1}) indicate that these selection rules have broken down completely and all states of the correct symmetry are seen in the spectrum, *but only in the neighbourhood of the expected C–O stretching transitions* This is typical of states with high vibrational energy in polyatomic molecules and represents a transition to a 'statistical' or 'chaotic' regime Here each state is mixed with every other state of the same symmetry by an essentially random, small amount

The result is shown in Figure 10, our zero-order model is shown in Figure 10a, consisting of two basic parts On the left is a single state involving only the C–O stretching motion which should show up strongly in the SEP spectrum and is therefore known as a *bright* state There are also many other vibrational states at this energy involving the many possible combinations of all the other modes in the molecule to which no transitions are expected, these are known as *dark* states Now the bright state will have a small matrix element mixing it with each of the dark states, and the net mixing will be roughly inversely proportional to the energy separation between the bright and the dark state as the variation in the matrix elements is relatively small This gives the levels shown in Figure 10b, where the bright state character has been shared out over the nearby dark states The amount of the bright state in each dark state is indicated by the width of the transition line, the result matches the form of the observed SEP spectra at high energies This mixing is normally only seen at high vibrational energy where the density of states is high, though it can show at low energies when there is a chance match in energy between two levels, this is known as *Fermi Resonance* [17] (Dense clumps of lines are not seen in the HCN case as the density of states is much lower, <1 per cm^{-1} even at 24000 cm^{-1}) An alternative way of looking at this is that the mixing between vibrational modes is such that the energy only stays localised in the initially prepared C–O bond for a short time, the width of the clumps (20–30 cm^{-1}) implies this is ~0 15 ps At the highest energies in the CH_3O spectra the line widths change as shown by Figure 9, from laser limited (~0 04 cm^{-1}) to >1 cm^{-1} This is probably due to dissociation into H + H_2CO as the threshold energy for this process is about 8400 cm^{-1}

Several other small polyatomic molecules have been studied

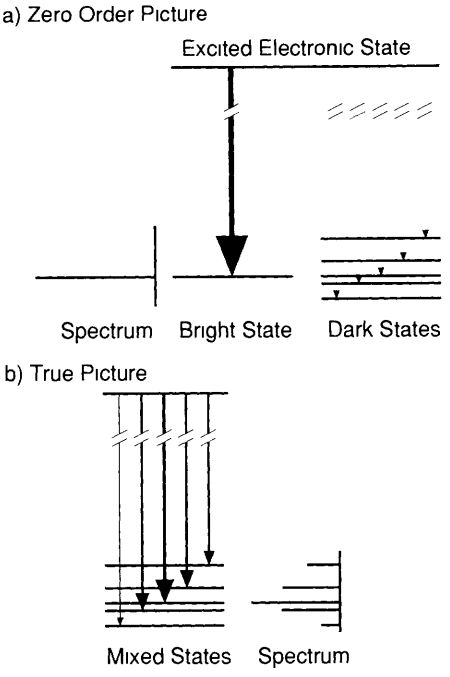

Figure 10 'Chaotic' vibrational energy levels

by SEP, including C_3, NCO, and C_2H_2 The reader is referred to more detailed reviews for further information [13 14] It is also worth mentioning another technique variously known as *degenerate four wave mixing* or *laser induced grating spectroscopy* [18] This technique relies on the interference between two laser beams of the same frequency generating a transient diffraction grating in the sample (manifested as a varying refractive index of the sample) A probe beam diffracted off this provides the detected signal While this technique is complicated to set up it is very promising for future work as the variant equivalent to SEP is potentially much more sensitive than SEP itself since there is no single resonant signal, thereby removing the requirement for difference techniques that limit the sensitivity of SEP

6 Van der Waals Molecules

The range and precision of the determinations of the potential energy surface illustrated above can be extended to cover the forces acting between molecules (intermolecular forces) as well as those acting within molecules (intramolecular forces) This is possible by taking spectra of weakly bound complexes held together by the weak forces that act between normal molecules These are known as Van der Waals molecules (after the forces involved) and include such species as Ar_2, ArHCl, $(HF)_2$, and ArOH It is important to emphasize that these molecules are not held together by strong chemical bonds and the binding energies are only of the order of 100 cm^{-1} for the non hydrogen-bonded complexes This means that the equilibrium concentration under normal conditions is very low and it is only in the low temperature, collision-free environment of a molecular beam that significant concentrations can be prepared The weak bonding also gives problems in the spectroscopy of these complexes as many of the approximations normally used in spectroscopic analysis break down There is, however, one important simplifying feature in the analysis the individual molecules making up the complex are little changed on complex formation and the use of the spectroscopic properties of the free molecules (transformed if required to the axis system of the complex) gives a good starting point to any analysis Perhaps the best example of what can be achieved is work on the ArHCl potential[19] which has produced a very detailed map of the potential as a function of all three internal coordinates

As is true of this paper in general, we cannot hope to provide anything approximating full coverage of the spectroscopy of

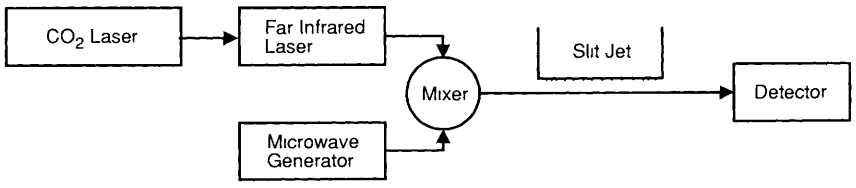

Figure 11 Outline of the apparatus for taking far infrared spectra of Van der Waals molecules

Van der Waals molecules, but can only highlight some interesting and topical areas Much of the early work involved microwave spectroscopy of these clusters, these of course yielded the equilibrium structure of the complex and, to a greater extent than microwave spectroscopy on normal molecules, information on the bonding in the complex This is because the weak bonds within the complex imply large zero-point motion which shows in the hyperfine constants and also as large centrifugal distortions A thorough discussion of the results that can be obtained in this way is provided in reference 20

6.1 Infra-red Spectroscopy

Just as for conventional molecules the best determination of the potential energy surface requires the measurement of a wide range of vibrational energy levels The weak bonds imply that there will be relatively few vibrational levels to measure but the low frequency implies that spectra must be taken in the technically difficult far infrared region For a species such as ArHCl similar information can, in fact, be obtained from near infrared spectra as the complex will give transitions in this region arising from the H–Cl stretch Combinations of this high frequency mode and the low frequency Van der Waals modes can readily be observed and are similar to pure Van der Waals mode spectra as the H–Cl vibration has relatively little effect on the complex

Taking infrared spectra of complexes is, in general, difficult as the spectra has to be taken in absorption which is far from ideal for the molecular beam sources that must be used for Van der Waals spectroscopy The short path length and relatively low concentration of the species of interest in a molecular beam mean that the attenuation of the laser beam is much too small to measure directly In fact little infrared spectroscopy has been performed in molecular beams, the standard methods of molecular beam spectroscopy normally rely on detecting a side effect of absorption, such as fluorescence or ionization, which occur on a true zero background making small changes much easier to detect These side effects are not present after infrared absorption, so special techniques must be used to enhance the sensitivity, we describe here the work of Saykally and co-workers on far infrared spectra,[21] though similar techniques have been used in the near infrared by Nesbitt and co-workers [22]

An outline of the far infrared apparatus used is shown in Figure 11, the key feature in this experiment is the use of a slit rather than a simple circular hole to produce the molecular beam The slit used in this study is 10 cm long by 25 μm wide, not only does this provide a much enhanced absorption path length but it also is more effective at generating Van der Waals clusters than an ordinary molecular beam This is because the pressure falls off less rapidly, being proportional to $1/x$ rather than $1/x^2$, where x is the distance from the nozzle (This is the difference between a point and a line source) As formation of Van der Waals molecules is a three-body process, the higher pressures encourage their formation Obtaining tuneable far infrared radiation is also tricky, the scheme shown here is to use a fixed frequency far infrared laser (pumped by a CO_2 laser) and mix the output of this with readily tuneable microwave radiation to give tuneable radiation in the far infrared The net result is a very sensitive spectrometer which has been used to take spectra of many Van der Waals molecules [21]

As an example consider work on the ArH_2O complex, nine vibrational bands have been measured for this complex in the far

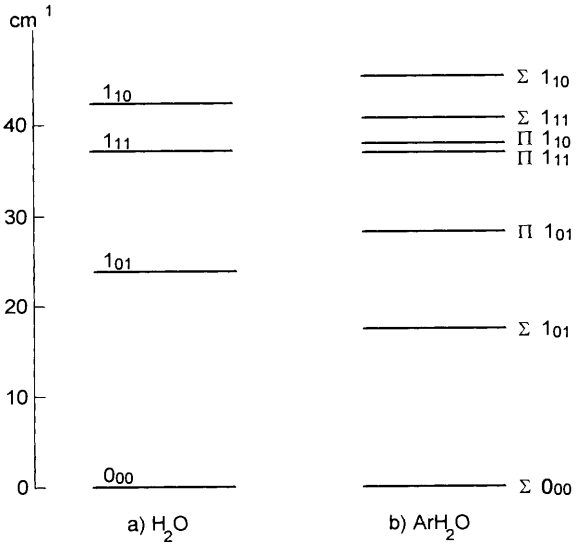

Figure 12 Schematic energy level diagram for H_2O and ArH_2O

infrared, together with five transitions for deuterated species Figure 12 shows the lower vibrational levels of ArH_2O This illustrates the unusual energy level patterns often found in Van der Waals complexes The H_2O is almost completely free to rotate within the complex (the zero-point energy is above the small barrier to rotation) so, instead of using the conventional bending vibrational quantum numbers, the asymmetric top quantum numbers (here 1_{11}, 1_{01}, 1_{10} and 0_{00}) are used to label the states For a free H_2O molecule (Figure 12a) these define the rotation of the molecule precisely, but in the complex the $2J + 1$ degeneracy is lifted, here giving Σ and Π components for $J = 1$ The diagram shows that the energy changes are not that large and so the free rotor states are providing quite a good guide as to where the states lie Not shown on this diagram are levels associated with stretching of the $Ar\cdots H_2O$ bond which behave in a more conventional manner Combining all the available information has lead to the 'AW2' surface [23] The most recent work in this area is now concentrating on Van der Waals trimers,[22] as these allow investigation of three-body forces These forces alter the interaction between two molecules when a third molecule is present, and are thought to be vital for the correct calculation of liquid and solid properties

6.2 Open Shell Complexes

The final topic to be considered is that of Van der Waals molecules where one of the partners is an open shell molecule or radical This is potentially very interesting as the open shell species introduces effects not present in closed shell molecules For example, if the uncomplexed molecule has an unfilled π orbital then the presence of another molecule can lift the π degeneracy giving two different electronic states

Spectra of Van der Waals radicals have mainly been taken by electronic (ultra-violet or visible) spectroscopy This was one of the methods used in early work on Van der Waals clusters, but it is only recently that it has become possible to take spectra of complexes of unstable species This is because of difficulties in

preparation – high concentrations of the unstable species must be produced in the presence of a large excess of inert gas. (Supersonic expansions typically work with < 5% of the species of interest in 1—20 atmospheres of inert gas.) This excludes some of the traditional methods for producing radicals, such as flames and microwave discharges. However these production difficulties have now been overcome and several open shell clusters have thus been studied.

The most fruitful work has been on ArOH. This was first made by photodissociating HNO_3 with a laser either just inside the supersonic nozzle (by Lester and coworkers[24]) or just outside the supersonic nozzle (by Heaven and co-workers[25]). The key point in these experiments is that the radical must be prepared in the high pressure region of the expansion where cooling collisions are frequent so that the energy released by the photodissociation process can be removed and the clusters formed. The apparatus is indicated schematically in Figure 13; the probe laser will typically be located 1 cm downstream of the nozzle. It has also been possible to prepare ArOH using an electric discharge operating in the high pressure region.[26] A spectrum of ArOH is shown in Figure 14; it is typical of electronic spectra of Van der Waals molecules in that it shows very strong signals due to the uncomplexed radicals, in this case from the $A^2\Sigma^+ - X^2\Pi$ transition in OH and much weaker signals from the complex. The small shift from the uncomplexed signal is typical as the electronic energy is not much affected by complex formation.

In fact ArOH has an unusually large change in the Van der Waals bond for this type of electronic excitation. The ground state binding energy is $\sim 100\ cm^{-1}$, typical for Ar complexes, but this increases to $\sim 1000\ cm^{-1}$ in the excited state, suggesting some incipient chemical bonding. This implies a change in the Van der Waals bond length and consequently a long progression in the excited state Van der Waals stretch. Enough bending levels are also observed to allow a reasonably complete determination of the excited state potential. The ground state has also been studied extensively, making use of stimulated emission pumping[24] which, as we saw above, has been so successfully applied to bound molecules. The change in geometry in the excited state of ArOH has allowed nearly all the bound vibrational levels in the ground state to be observed and the SEP measurements, combined with microwave spectra, has lead to the detailed determination[27] of the ground state potential shown in Figure 15. The minimum is at the linear Ar–H–O configuration, with a secondary minimum ($44\ cm^{-1}$ higher) at the other linear configuration. Unfortunately the details of the most interesting feature, the lifting of the π degeneracy in the ground state is still unclear, but it seems that there is a difference of $\sim 10\ cm^{-1}$ between the energies of the ArOH molecule with the odd electron in the in-plane and out-of-plane orbitals.[28]

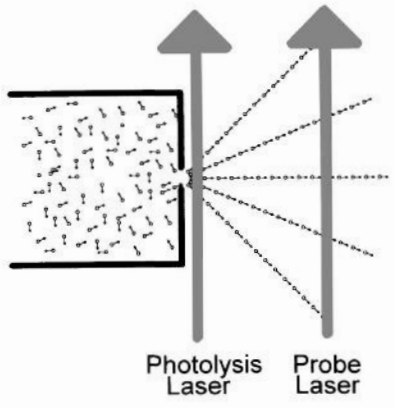

Figure 13 Apparatus for preparing Van der Waals complexes of transient species.

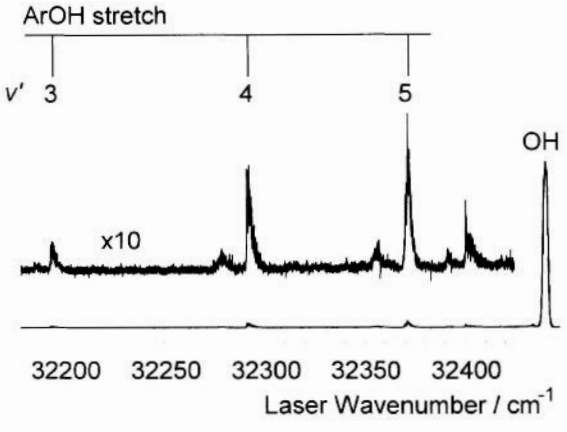

Figure 14 Spectrum of ArOH adjacent to the $A^2\Sigma^+ - X^2\Pi$ transition on OH. The OH signal, even on the lower trace, is strongly saturated.

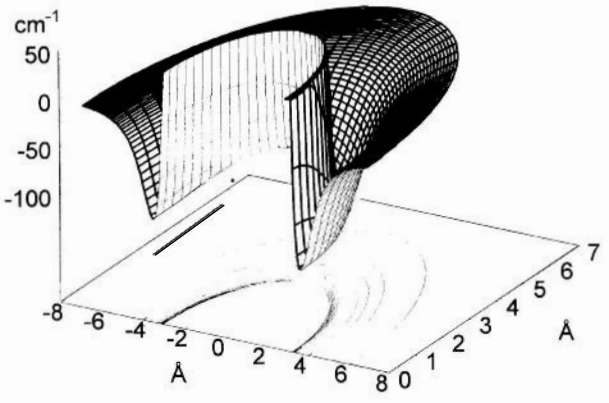

Figure 15 Potential energy surface for the $X^2\Pi$ state of ArOH, showing how the energy changes as the Ar atom moves round the OH sub-unit for fixed O–H bond length.

Several other open shell complexes have been studied by similar methods;[29] one recent experiment[30] on the $A^1\Pi$–$X^1\Sigma^+$ transition in ArAlH found, in contrast to the ArOH case, the π degeneracy very strongly lifted in the excited state. The in plane and out of plane orbitals differ in energy by $> 100\ cm^{-1}$ and the complex has a completely different equilibrium geometry depending on which of the two π orbitals is populated.

7 Conclusion

I hope I have given a flavour of the variety of experiments that can be performed in order to measure a wide variety of vibrational levels of a molecule, and the quality of the potential energy surfaces that can be extracted from such data. One very general comment can be made: the best determinations come from combining data from several sources; it is rare that a single experiment can provide all the required data.

8 References

1 R. N. Dixon, *Chem. Soc. Rev.*, 1994, **23**, 375.
2 J. M. Hollas, *Chem. Soc. Rev.*, 1993, **22**, 371.
3 S. Gerstenkorn and P. Luc, 'Atlas du spectra d'absorption de la molecule d'iode, 14800–20000 cm^{-1}', Centre National de la Recherche Scientifique, Paris, 1978.
4 D. M. Hirst, 'Potential Energy Surfaces', Taylor and Francis, London, 1985, p. 15.
5 J. Tellinghuisen, *Comp. Phys. Commun.*, 1974, **6**, 221.
6 J. Tennyson and S. Miller, *Chem. Soc. Rev.*, 1992, **21**, 91.
7 S. Carter, I. M. Mills, and N. C. Handy, *J. Chem. Phys.*, 1993, **99**, 4379.
8 A. R. Skinner and D. W. Skinner, *Am. J. Phys.*, 1980, **48**, 8.

9 J M Allen, M N R Ashfold, R J Stickland, and C M Western, *Mol Phys*, 1991, **74**, 49
10 D L Andrews, 'Lasers in Chemistry', Springer Verlag, 1986
11 J D Tobiason, A L Utz, E L Sibert III, and F F Crim, *J Chem Phys*, 1993, **99**, 5762
12 D Romanini and K K Lehmann, *J Chem Phys*, 1993, **99**, 6287
13 F J Northrup and T J Sears, *Annu Rev Phys Chem*, 1992, **43**, 127
14 C E Hamilton, J L Kinsey, and R W Field, *Annu Rev Phys Chem*, 1986, **37**, 493
15 D M Jonas, X Yang, and A M Wodtke, *J Chem Phys*, 1992, **97**, 2284
16 A Geers, J Kappert, F Temps, and J W Wiebrecht, *J Chem Phys*, 1994, **101**, 3618, 3634
17 G Herzberg, 'Molecular Spectra and Molecular Structure II Infrared and Raman Spectra of Polyatomic Molecules', Van Nostrand Reinhold, 1945
18 G Hall and B J Whitaker, *J Chem Soc, Faraday Trans*, 1994, **90**, 1
19 J M Hutson, *J Phys Chem*, 1992, **96**, 4237
20 A C Legon and D J Millen, *Chem Soc Rev*, 1992, **21**, 71
21 R C Cohen and R J Saykally, *J Phys Chem*, 1992, **96**, 1024
22 M A Suhm and D J Nesbitt, *Chem Soc Rev*, 1995, **24**, 45
23 R C Cohen and R J Saykally, *J Chem Phys*, 1993, **98**, 6007
24 M T Berry, R A Loomis, L C Giancarlo, and M I Lester, *J Chem Phys*, 1992, **96**, 7890
25 W M Fawzy and M C Heaven, *J Chem Phys*, 1990, **92**, 909
26 S K Bramble and P A Hamilton, *Chem Phys Lett*, 1990, **170**, 107
27 M -L Dubernet and J M Hutson, *J Chem Phys*, 1993, **99**, 7477
28 M I Lester, *Faraday Discuss Chem Soc*, 1994, **97**, 422
29 M C Heaven, *J Phys Chem*, 1993, **97**, 8567
30 M Yang, M H Alexander, S Gregurick, and P J Dagdigian, *J Chem Phys*, 1995, **102**, 2413, 2426